INDIAN JOURNAL OF SCIENCE AND TECHNOLOGY

RESEARCH ARTICLE

# Effect of Uneven Heat Sink/Source and Nonlinear Radiation on Hydromagnetic Casson Fluid Flow Past an Inclined Elongating Sheet

**C Sulochana**[1]*, **Savita** [1]

**1** Department of Mathematics, Gulbarga University, Gulbarga, 585106, Karnataka, India

OPEN ACCESS

**Received:** 11-10-2022

**Accepted:** 30-11-2022

**Published:** 27-12-2022

**Citation:** Sulochana C, S (2022) Effect of Uneven Heat Sink/Source and Nonlinear Radiation on Hydromagnetic Casson Fluid Flow Past an Inclined Elongating Sheet. Indian Journal of Science and Technology 15(48): 2716-2726. https://doi.org/10.17485/IJST/v15i48.2008

* **Corresponding author**.

math.sulochana@gmail.com

**Funding:** None

**Competing Interests:** None



Published By Indian Society for Education and Environment (iSee)

**ISSN**
Print: 0974-6846
Electronic: 0974-5645

## Abstract

**Objectives:** The present article investigates the steady flow of hydromagnetic Casson fluid flow past an inclined stretched sheet with the existence of nonlinear radiation and Joule heating effects. **Methods:** A numerical model is established and then solved using the BVP4c MATLAB technique. **Findings:** In this present work we described about the influence of the Grashof number, non-uniform heat source, Biot number, Casson fluid parameter, hydrodynamics, nonlinear radiation, chemical reaction, local Grashof number and Schmidt number parameters on the flow of mass and rate of heat transport was discussed through tabular result and graphs. It is clear that the rate of heat transport decreases with Joule heating and is higher with an increase in Biot numbers. Increases the amount of thermophoresis parameter and decreases with the rate of heat transport. **Novelty:** To the best extent of the authors' belief so far, no attempt is made to inspect the flow, thermal and mass transfer of uneven heat sink/source and non-linear radiation on hydromagnetic and embedded with the viscous dissipation, thermophoresis, Brownian diffusion, Joule heating and Casson fluid.

**Keywords:** NonUniform Heat Sink/Source; Casson Fluid; Joule Heating; NonLinear Radiation; Hydromagnetic

## 1 Introduction

The significance of non-Newtonian fluid importance is being found in several branches of applications and engineering, especially in the design of solid matrix heat transportation, petroleum cooling etc. Haroon et al[(1)] examined the flow of non-Newtonian MHD incompressible fluid flow over a vertical stretched sheet. Hamid et al.[(2)] studied heat transit of the hydrodynamic on the flow of variable incompressible non-Newtonian fluid flow over a shrinking sheet. Anwar et al.[(3)] probed the heat and mass transit the Casson Nano material was generated by the inclined stretching surface. Anantha Kumar et al.[(4)] numerically examined the impact of hydromagnetic on Casson fluid with heat sink/source through a shrinking sheet. Swain et al[(5)] have described the flow of MHD Casson nanofluid past a stretched surface and in the presence of a Joule heating effect.

Joule heating is representative of Ohmic heating due to its connection to the Ohm's Law and it is the base for a number of practical applications like electric fuses and so forth. Kumar & Srinivas[6] have discussed the magneto-hydrodynamic nanofluid flow over a shrinking surface and they have observed that the higher the velocity of the fluid with the lower local Grashof number. Samuel[7] investigated the impact of hydromagnetic on Ohmic heating and viscous fluid on a porous sheet. Jagadeeshwar and Srinivasacharya[8] have numerically examined the heat transit of the Joule heating with convective boundary conditions on MHD fluid flow and they observed that the lower in Nusselt number as well as the higher in Biot number. The impact of Ohmic heating under the consideration of hydrodynamic flow through a stretching plate was deliberated by Gholinia et al.[9]. The rate of heat transit for the flow of natural convective boundary layer surface on hydrodynamic Casson fluid through an elongating sheet was reported by Das[10].

The Ohmic heating and nonlinear radiation of the heat transporting the hydromagnetic fluid flow over a stretchable surface were presented by Tarakaramu and Narayana[11]. Sharma and Shaw[12] have reported that the Casson-MHD fluid flow of heat and mass transported, under the consideration of thermo-diffusion and non-linear radiation. Parmar and Jain[13] have reported the hydromagnetic Williamson fluid flow of the convective slip flow past an inclined shrinking sheet. The natural convection flow of thermophoresis and Brownian diffusion in hydromagnetic flow due to a nonlinear stretchable flow in the existence of Ohmic heating was influenced by Patel and Singh[14]. After that, Ebrahem et al.[15] studied heat transit, the natural convection flow of Casson fluid on Oldroyd-B flow through a shrinking sheet. Dawar et al.[16] reported the magnetized and non-magnetized flow of the Casson fluid and microorganisms. Durga et al.[17] discussed the study of CO2 and graphene oxide embedded with the TiO2 nanotubes. Sunder et al.[18] the effect of an uneven heat source/sink on 2D MHD Casson fluid through an infinite plate with the presence of Ohmic heating. Sharma and Gandhi[19] have discussed both the combined effect of Joule heating and non-uniform heat source/sink on hydrodynamic convective flow through a vertical stretching/shrinking sheet.

To the best of our knowledge, no author has inquired about the impact of uneven heat sink/source and nonlinear radiation on hydromagnetic Casson fluid flow past an inclined elongating stretching sheet. The governing equations of flow momentum, heat and mass transport are characterized by a set of partial differential equations. Later, these equations are transformed into ordinary differential equations by utilizing proper similarity functions and are thereby resolved numerically by the Runge–Kutta technique. The effects of different relevant physical parameters on the flow, skin friction, Nusselt and Sherwood number designations are discussed through graphical outputs and numerical values are through the tables.

## 2 Basic Equation

Consider a steady 2D flow of an incompressible Casson fluid flow which is produced by the inclination of the surface at an angle $\alpha$ vertically. $U_\infty(x) = 0, U_w(x) = bx$are the free stream stretched velocities respectively. Also the Brownian diffusion and thermophoresis are taken into account. The x-axis moves along the stretching sheet (see Figure 1). $C_w$ is the concentration wall and $T_w$is taken as temperature wall. The ambient fluid $T_\infty$&$C_\infty$ is taken respectively as y tends to infinity at the stretchable flow. The Casson fluid flow of an incompressible and rheological equation of mode for an isotropic is as follows:

$$\tau_{ij} = \begin{cases} \left(\mu_B + \dfrac{P_y}{\sqrt{2\pi}}\right) 2e_{ij}\pi > \pi \\ \left(\mu_B + \dfrac{P_y}{\sqrt{2\pi_c}}\right) 2e_{ij}\pi_c > \pi \end{cases} \tag{1}$$

Where $P_y$-yield stress of the fluid, $\mu_B$- plastic dynamic viscosity of non-Newtonian fluid $\pi = e_{ij}e_{ij}$ $\pi$ - product of the component of deformation rate with itself and $e_{ij}$are the component of the deformation $(i, j)^{th}, \pi_c$−critical value of $\pi$ based on non-Newtonian model. With respect to the above conditions, we can write the governing equations of the flow as[20]

$$\frac{\partial u}{\partial x} + \frac{\partial v}{\partial y} = 0 \tag{2}$$

$$u\frac{\partial u}{\partial x} + v\frac{\partial u}{\partial y} = \nu\left(1 + \frac{1}{\beta}\right)\frac{\partial^2 u}{\partial y^2} + \left((T - T_\infty)g\beta_1 + (C - C_\infty)g\beta_2\right)\mathrm{Cos}\,\alpha - \frac{\sigma B_0^2}{\rho}u \tag{3}$$

$$\begin{aligned} u\frac{\partial T}{\partial x} + v\frac{\partial T}{\partial y} =& \alpha\frac{\partial^2 T}{\partial y^2} + \frac{\nu}{\rho C_P}\left(1 + \frac{1}{\beta}\right)\left(\frac{\partial u}{\partial y}\right)^2 + \frac{\sigma B_0^2}{\rho C_P}u^2 + \frac{q''}{\rho C_p} - \frac{1}{\rho C_P}\frac{\partial q_r}{\partial y} \\ &+ \tau\left[D_B\frac{\partial C}{\partial y}\frac{\partial T}{\partial y} + \frac{D_T}{T_\infty}\left(\frac{\partial^2 T}{\partial y^2}\right)\right] \end{aligned} \tag{4}$$

$$u\frac{\partial C}{\partial x} + v\frac{\partial C}{\partial y} = D_B\frac{\partial^2 C}{\partial y^2} + \frac{D_T}{T_\infty}\frac{\partial^2 T}{\partial y^2} - (C - C_\infty)K_C \tag{5}$$

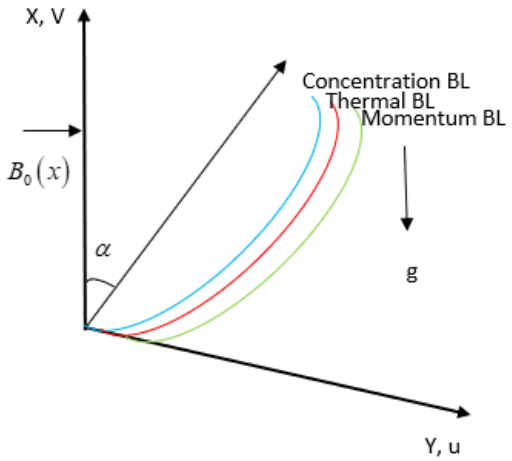


**Fig 1.** Flow configuration

With initial BCs:

$$\left.\begin{aligned} &u = bx, v = v_w, K\frac{\partial T}{\partial y} = -h\left(T - T_w\right), C = C_w \text{ at } y = 0 \\ &u \to 0, T \to T_\infty, C \to C_\infty \text{ as } \quad y \to \infty \end{aligned}\right\} \tag{6}$$

Here $g$is the gravitational constant, $v$is the kinematics viscosity,$bx$ is assumed as wall velocity, $v_w$is the Suction velocity, $T, C$is the temperature and concentration fluid, $B_0$is the magnetic field, $K_C$is the chemical reaction,$\beta = \mu_B\left(\frac{2\pi_C}{P_y}\right)$ is taken as Casson fluid parameter, $\beta_1\beta_2$are the concentration, The velocity components for the$u$&$v$ are $x, y$ directions and thermal expansion of the fluid, $D, K, Cp$ and $\rho$ are the diffusion term, specific heat capacity, conductivity of the thermal. Now introducing the temperature$\theta(\eta) = \frac{(T-T_\infty)}{(T_w-T_\infty)}$ in the term of $T = T_\infty\left(1 + (\theta_w - 1)\,\theta\right)$

Here$\theta_w = \frac{T_w}{T_\infty}$ is taken as thermal parameter. The1st term on RHS side of equation (4) can be expressed as

$\alpha\frac{\partial}{\partial y}\left\{\frac{\partial T}{\partial y}\left(1 + R\left(1 + (\theta_w - 0)\,\theta\right)^3\right)\right\}$

Where $R = -\frac{16\sigma^* T_\infty^3}{3KK^*}$

The parameter of non-uniform heat sink/source is,

$$q''' = \frac{KU_\infty(x,t)}{xv}\left[\left(T_w - T_\infty\right)A^* f' + B^*\left(T - T_\infty\right)\right] \tag{7}$$

In the above expression, the time dependent and space of heat sink/source are $A^*, B^*$ .

The similarity variables are,

$$\begin{aligned} &\eta = y\sqrt{\frac{b}{v}}, \psi = \sqrt{bv}xf(\eta), \phi(\eta) = \frac{C - C_\infty}{C_w - C_\infty} \\ &\theta(\eta) = \frac{T - T_\infty}{T_w - T_\infty} \end{aligned} \tag{8}$$

Here $u = \frac{\partial\psi}{\partial y}$ and $v = -\frac{\partial\psi}{\partial x}$, $\psi$, is stream function, which satisfies the continuity equation (2), and by using these definitions, we get,

$$u = bvxf'(\eta), \quad v = -\sqrt{bv}f(\eta) \tag{9}$$

Substituting the equations (8)-(9) into the equations (3,4,5 and 6) above the transformed equations as becomes,

$$\left(1+\frac{1}{\beta}\right)f'''+ff''+f'^2-(Gr\theta+Grc\phi)\,\mathrm{Cos}\,\alpha+Mf'=0 \tag{10}$$

$$\frac{\theta''}{\mathrm{Pr}}\left[\left(1+R\left(1+(\theta_w-1)\,\theta\right)^3\right)\theta'\right]'+f\theta'-\left(1+\frac{1}{\beta}\right)Ecf''^2-MEcf'^2 \\ -Nb\theta'\phi'-Nt\theta'^2-\left[Af'+B\theta\right]=0 \tag{11}$$

$$\phi''+Scf\phi'-ScK\phi-\frac{Nt}{Nb}=0 \tag{12}$$

With BCEs

$$\left.\begin{array}{l} f(0)=f_w, f'(0)=1, \theta'(0)=-Bi(1-\theta(0)), \phi(0)=1, \text{ at } \eta=0 \\ f'(\infty)\to 0, \theta(\infty)\to 0, \phi(\infty)\to 0, \text{ as } \eta\to\infty \end{array}\right\} \tag{13}$$

The nondimensional parameters are Schmidt number, chemical reaction, Eckert number, Grashof and Local Grashof number, magnetic parameter, suction parameter, Grashof number, and Prandtl number.

Where,

$$M=\frac{\sigma B_0^2}{\rho b}, Sc=\frac{v}{D}, Ec=\frac{u^2}{C_P\left(T_w-T_\infty\right)}, K=\frac{K_C}{b}, Gr=\frac{g\beta_1\left(T_w-T_\infty\right)}{bu}, \\ Grc=\frac{g\beta_2\left(C_w-C_\infty\right)}{bu}, \mathrm{Pr}=\frac{\mu C_P}{K}, f_w=-\frac{v_w}{\sqrt{bv}}, \theta_w=\frac{T_w}{T_\infty} \tag{14}$$

The Skin frication, Nusselt and Sherwood numbers respectively,

$$\mathrm{Re}_x^{1/2}C_f=\left(1+\frac{1}{\beta}\right)f''(0), \\ Nu_x\,\mathrm{Re}_x^{1/2}=-\theta'(0), \\ Sh_x\,\mathrm{Re}_x^{1/2}=-\phi'(0). \tag{15}$$

## 3 Results and Discussion

The effect of governing non-dimensionless parameters on nonlinear radiation, Casson parameter, magnetic field, chemical reaction, non-uniform heat source, Schmidt number, thermophoresis, Eckert number and Brownian diffusion are evaluated. And also, the effect of dimensionless governing profile computed on the momentum, thermal and concentration. Using the numerical method with bvp4c embedded in the MATLAB software scheme, in this present study the fixed values of the governing profiles are taken as $\mathrm{Pr}=0.71, R=0.1$ ,

$\theta_w=1.1$, $M=1$, $Bi=1$, $Ec=1$, $Kc=0.5$, $A\&B=0.01$, $Nt$ & $Nb=0.2$, $\beta=0.5$, $\alpha=\frac{\pi}{2}$

Figure 2 scrutinized the influence of magnetic profile on velocity. In the presence of electrically conducting fluid in a magnetic field, it influences a force known as the Lorentz force, which opposes the flow. The velocity parameter decreases with the magnetic profile and the opposite phenomenon exists in the case of concentration and temperature.

The thermal curve that are affected by the nonlinear radiation as cited in Figure 3, the concentration parameter has been shown to decrease with the nonlinear radiation profile and this is appropriate with the empirical observation that the concentration boundary layer decrease as nonlinear radiation decreases. The impact of the Eckert number on thermal parameter is displayed in Figure 4. It is noticed that the thermal profile is lower with the corresponding boundary layer surface is thinner.

The impact of Brownian diffusion on the concentration and temperature parameters for the various distributions is seen in Figures 5 and 6. The concentration parameter increases marginally because of the increased values of Brownian motion. This is due to the Brownian motion increasing as the temperature parameter decreases.

Figures 7 and 8 described the impact of thermophoresis on concentration and temperature profiles for the various distributions and it is seen that the concentration parameter is lowest with thermophoresis profile and highest with the thermal parameter and boundary layer surface.

The Grashof and local Grashof numbers on momentum parameters are displayed in Figures 9 and 10. From these plots, the momentum parameters decrease by decreasing the thermal Grashof number and higher in the values of mass Grashof number.

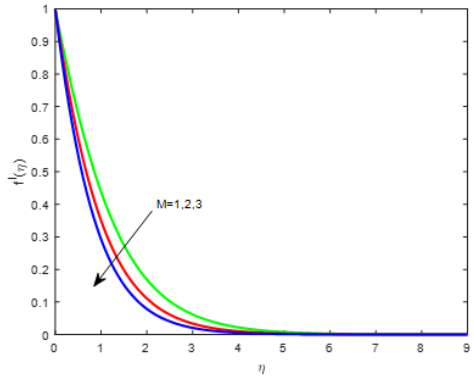


**Fig 2.** Effect of $M$ over $f'(\eta)$

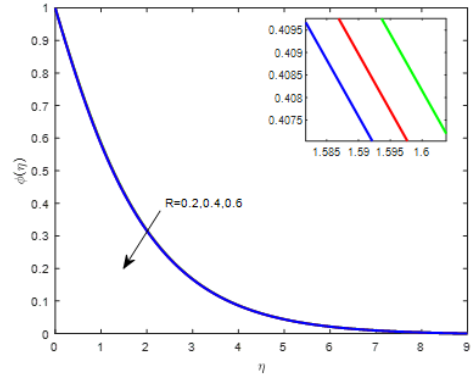


**Fig 3.** Effect of $R$ over $\phi(\eta)$

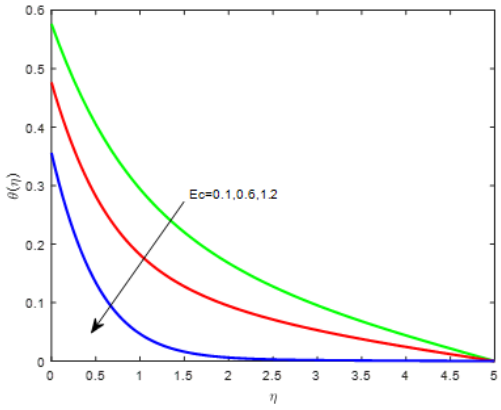


**Fig 4.** Effect of $Ec$ over $\theta(\eta)$

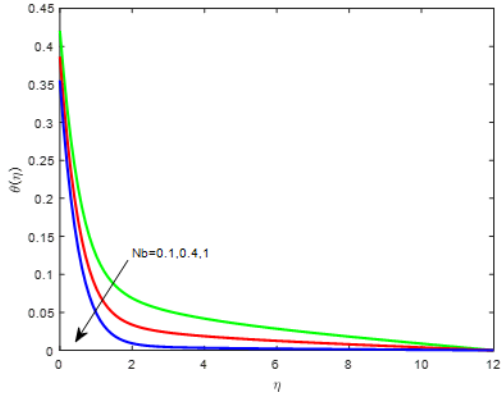


**Fig 5.** Effect of $Nb$ over $\theta(\eta)$

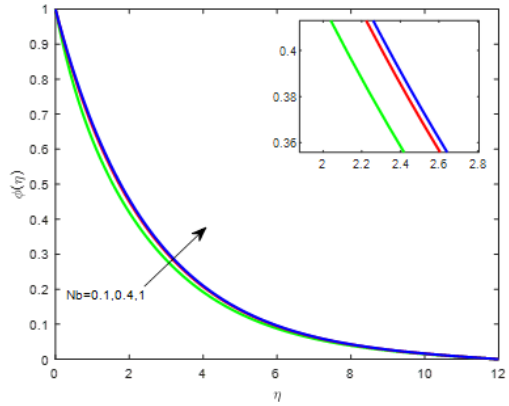


**Fig 6.** Effect of $Nb$ over $\phi(\eta)$

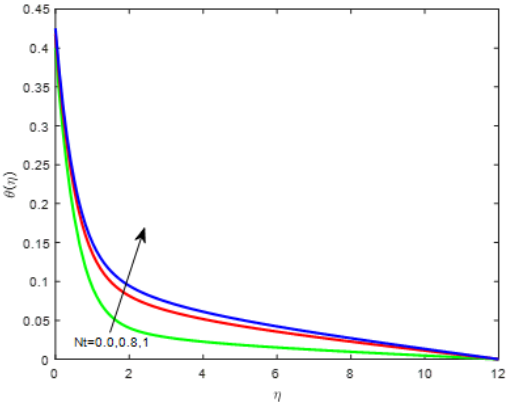


**Fig 7.** Effect of $Nt$ over $\theta(\eta)$

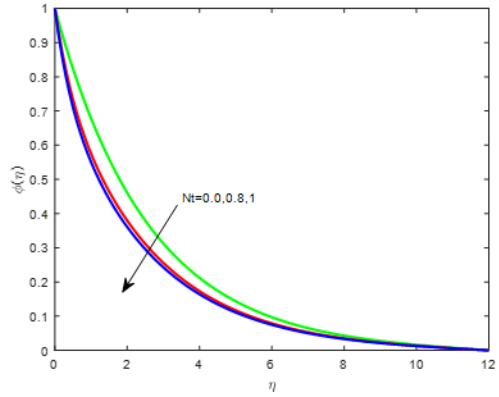


**Fig 8.** Effect of $Nt$ over $\phi(\eta)$

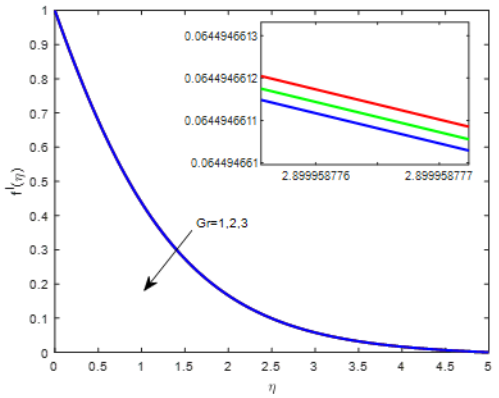


**Fig 9.** Effect of $Gr$ over $f'(\eta)$

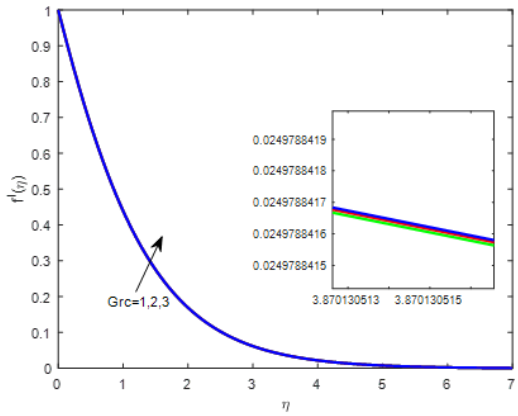


**Fig 10.** Effect of $Grc$ over $f'(\eta)$

Also, it was noticed that the thermal Grashof number have increased by increasing the number of local Grashof. Increasing the Grashof number for the rate of mass transport increases the friction factor and reduces the Nusselt number.

The influence of non-uniform heat source /sink on the thermal profile is shown in Figures 11 and 12. Figure 11, thermal in the boundary layer produces the thermal energy and leads to a lower non-uniform heat sink/source with the temperature profile and in Figure 12 it is clear that the thermal boundary layer increases with the thermal profile.

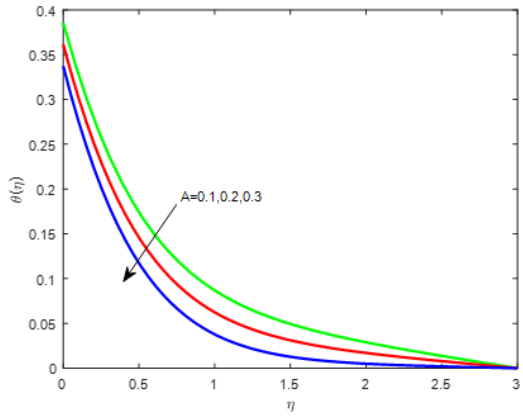


**Fig 11.** Effect of $A$ over $\theta(\eta)$

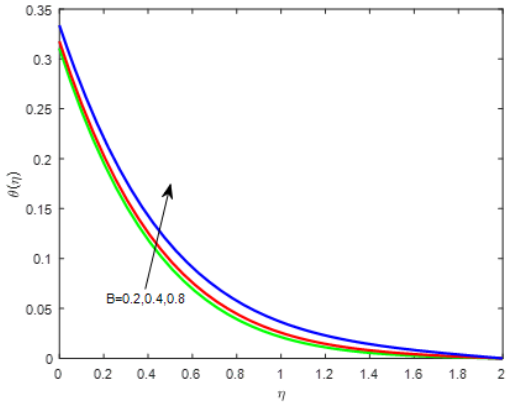


**Fig 12.** Effect of $B$ over $\theta(\eta)$

Figures 13 and 14 are the influence of concentration parameters for the different values of chemical reaction and Schmidt number. It is clear that the chemical reaction and Schmidt number increases with decreasing flow of the concentration parameters. This validates that the heavier diffusing species have a greater retarding effect on concentration parameters of the flow field.

The influences of Casson fluid profile are displayed on the momentum field as shown in Figure 15, respectively. From Figure 15, it is noticed that by increasing the Casson fluid profile, velocity has decreased. In view, a rise in the Casson fluid profile caused the rise in fluid viscosity and it is also noticeable that the highest viscosity results in a decrease in velocity. The impact of different profiles on the mass and heat transport and skin factor are displayed in Table 1. In the table, it is seen that an improvement in the quantity of the magnetic field profile comes in a decline in physical quantities of the flow of the friction factor, but a rise in heat transit and increases in the amount of magnetic field and thermophoresis results in an enhancement of the Nusselt number.

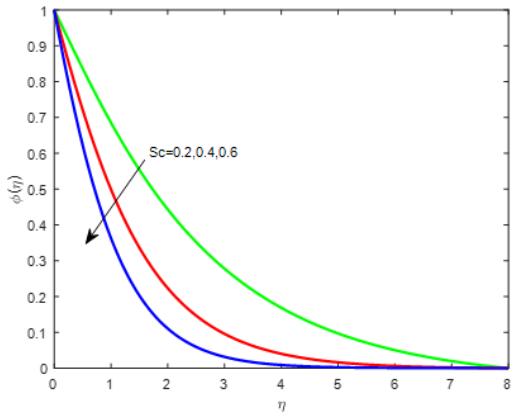


**Fig 13.** Effect of $Sc$ over $\phi(\eta)$

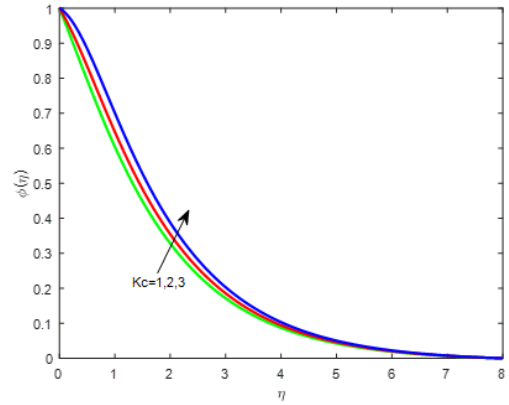


**Fig 14.** Effect of $Kc$ over $\phi(\eta)$

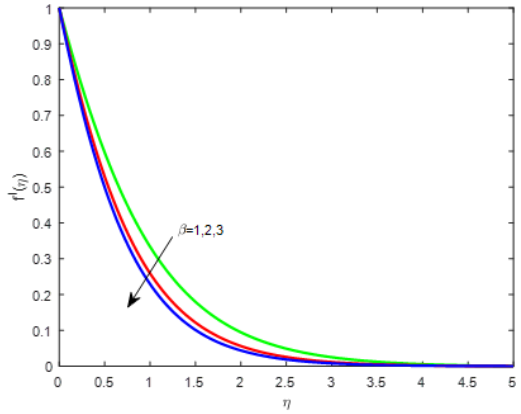


**Fig 15.** Effect of $\beta$ over $f'(\eta)$

**Table 1.** The Results $f'(\eta)$, $-\theta(\eta)$ and $-\phi(\eta)$ for the different physical parameters

| $M$ | Nb | $Nt$ | $Q$ | $Ec$ | $\beta$ | $Bi$ | $f'(\eta)$ | $-\theta(\eta)$ | $-\phi(\eta)$ |
|---|---|---|---|---|---|---|---|---|---|
| 1 | | | | | | | -0.714724 | 0.543365 | 0.460178 |
| 2 | | | | | | | -0.953325 | 0.538723 | 0.435217 |
| 3 | | | | | | | -1.138898 | 0.536769 | 0.418481 |
| | 0.1 | | | | | | -0.714715 | 0.579469 | 0.526032 |
| | 0.4 | | | | | | -0.714715 | 0.613483 | 0.420728 |
| | 1 | | | | | | -0.714715 | 0.644786 | 0.401296 |
| | | 0.0 | | | | | -0.714715 | 0.600136 | 0.387370 |
| | | 0.8 | | | | | -0.714715 | 0.581995 | 0.715754 |
| | | 1 | | | | | -0.714715 | 0.574566 | 0.822131 |
| | | | 0.2 | | | | -0.714724 | 0.501000 | 0.466158 |
| | | | 0.4 | | | | -0.714724 | 0.433288 | 0.475426 |
| | | | 0.6 | | | | -0.714724 | 0.382824 | 0.482109 |
| | | | | 0.1 | | | -0.714855 | 0.343537 | 0.495345 |
| | | | | 0.2 | | | -0.714855 | 0.366157 | 0.492034 |
| | | | | 0.3 | | | -0.714855 | 0.388866 | 0.488704 |
| | | | | | 1 | | -0.942880 | 0.563374 | 0.459988 |
| | | | | | 2 | | -1.155213 | 0.565431 | 0.443039 |
| | | | | | 3 | | -1.257832 | 0.565746 | 0.436218 |
| | | | | | | 1 | -0.714855 | 0.550307 | 0.464872 |
| | | | | | | 2 | -0.714855 | 0.658589 | 0.456947 |
| | | | | | | 3 | -0.714855 | 0.705336 | 0.453484 |

## 4 Conclusion

The study presents the hydromagnetic non-linear radiation and Casson fluid flow past an inclination of the stretched surface. It considered the non-linear radiation, Joule heating, chemical reaction, non-uniform heat sink/source and Schmidt number using the Runge-Kutta method. Some prominent findings are listed below:

- Sherwood numbers decrease as Brownian motion and non-uniform heat source and Schmidt number parameters decrease.
- The temperature parameter reduces the rate of mass transit and improves the non-uniform heat sink/source.
- Increasing the thermophoresis profile decreases the rate of heat transport.
- Increasing the magnetic field profile lowers the friction factor, Sherwood number and Nusselt number and it raises the skin factor.
- Brownian diffusion increases in the concentration parameter and decreases with the thermal boundary layer.

## References


1) Rasheed HU, Islam S, Zeeshan, Khan W, Khan J, Abbas T. Numerical modeling of unsteady MHD flow of Casson fluid in a vertical surface with chemical reaction and Hall current. *Advances in Mechanical Engineering*. 2022;14(3). Available from: https://doi.org/10.1177/16878132221085429.
2) Hamid M, Usman M, Khan ZH, Ahmad R, Wang W. Dual solutions and stability analysis of flow and heat transfer of Casson fluid over a stretching sheet. *Physics Letters A*. 2019;383(20):2400–2408. Available from: https://doi.org/10.1016/j.physleta.2019.04.050.
3) Anwar MI, Rafique K, Misiran M, Shehzad SA. Numerical study of hydrodynamic flow of a Casson nanomaterial past an inclined sheet under porous medium. *Heat Transfer-Asian Research*. 2020;49(1):307–334. Available from: https://doi.org/10.1002/htj.21614.
4) Kumar A, Sugunamma K, Sandeep V, N. Effect of thermal radiation on MHD Casson fluid flow over an exponentially stretching curved sheet. *Journal of Thermal Analysis and Calorimetry*. 2020;140(5):2377–2385. Available from: https://doi.org/10.1007/s10973-019-08977-0.
5) Swain K, Mishra M, Kumari A. Numerical study of Casson nanofluid over an elongated surface in presence of Joule heating and viscous dissipation: Buongiorno model analysis. . Available from: https://doi.org/10.22059/JCAMECH.2022.347011.745.
6) Kumar B, Srinivas S. Unsteady hydromagnetic flow of eyring-powell nanofluid over an inclined permeable stretching sheet with Joule Heating and thermal radiation. *Journal of Applied and Computational Mechanics*. 2020;6(2):259–270. Available from: https://doi.org/10.22055/JACM.2019.29520.1608.
7) Samuel DJ, Fayemi IA. Variable Viscosity and Chemical Reaction Effects on MHD Flow of Radiative Fluid Past a Stretching Sheet in the Presence of Joule Heating. 2022. Available from: https://doi.org/10.9734/arjom/2021/v17i1230346.

8) Srinivasacharya D, Jagadeeshwar P. Effect of Joule heating on the flow over an exponentially stretching sheet with convective thermal condition. *Mathematical Sciences*. 2019;13(3):201–211. Available from: https://doi.org/10.1007/s40096-019-0290-8.
9) Gholinia M, Hoseini ME, Gholinia S. A numerical investigation of free convection MHD flow of Walters-B nanofluid over an inclined stretching sheet under the impact of Joule heating. *Thermal Science and Engineering Progress*. 2019;11:272–282. Available from: https://doi.org/10.1016/j.tsep.2019.04.006.
10) Das UJ. MHD mixed convective slip flow of Casson fluid over a porous inclined plate with Joule heating, viscous dissipation and thermal radiation. 2021.
11) Tarakaramu N, Narayana PVS. Nonlinear Thermal Radiation and Joule Heating Effects on MHD Stagnation Point Flow of a Nanofluid Over a Convectively Heated Stretching Surface. *Journal of Nanofluids*. 2018;8(5):1066–1075. Available from: https://doi.org/10.1166/jon.2019.1651.
12) Sharma RP, Shaw S, Non. MHD Non-Newtonian Fluid Flow past a Stretching Sheet under the Influence of Non-linear Radiation and Viscous Dissipation. 2022. Available from: https://doi.org/10.22055/JACM.2021.34993.2533.
13) Parmar A, Jain S. Unsteady Convective Slip Flow of Inclined Magnetohydrodynamics Williamson Fluid with Non-Linear Radiation and Heat Source Past an Inclined Stretching Sheet. *Journal of Nanofluids*. 2019;8(3):640–650. Available from: https://doi.org/10.1166/jon.2019.1606.
14) Patel HR, Singh R. Thermophoresis, Brownian motion and non-linear thermal radiation effects on mixed convection MHD micropolar fluid flow due to nonlinear stretched sheet in porous medium with viscous dissipation, joule heating and convective boundary condition. *International Communications in Heat and Mass Transfer*. 2019;107:68–92. Available from: https://doi.org/10.1016/j.icheatmasstransfer.2019.05.007.
15) Algehyne EA, Aldhabani MS, Saeed A, Dawar A, Kumam P. Mixed convective flow of Casson and Oldroyd-B fluids through a stratified stretching sheet with nonlinear thermal radiation and chemical reaction. *Journal of Taibah University for Science*. 2022;16(1):193–203. Available from: https://doi.org/10.1080/16583655.2022.2040281.
16) Dawar A, Shah Z, Alshehri HM, Islam S, Kumam P. Magnetized and non-magnetized Casson fluid flow with gyrotactic microorganisms over a stratified stretching cylinder. *Scientific Reports*. 2021;11(1):1–14. Available from: https://doi.org/10.1038/s41598-021-95878-8.
17) Devi AD, Pushpavanam S, Singh N, Verma J, Kaur MP, Roy SC. Enhanced methane yield by photoreduction of CO2 at moderate temperature and pressure using Pt coated, graphene oxide wrapped TiO2 nanotubes. *Results in Engineering*. 2022;14:100441. Available from: https://doi.org/10.1016/j.rineng.2022.100441.
18) Ram MS, Ashok N, Salawu SO, Shamshudin MD. Significance of cross diffusion and uneven heat source/sink on the variable reactive 2D Casson flowing fluid through an infinite plate with heat and Ohmic dissipation. . Available from: https://doi.org/10.1080/02286203.2022.2084007.
19) Sharma BK, Gandhi R. Combined effects of Joule heating and non-uniform heat source/sink on unsteady MHD mixed convective flow over a vertical stretching surface embedded in a Darcy-Forchheimer porous medium. *Propulsion and Power Research*. 2022;11(2):276–292. Available from: https://doi.org/10.1016/j.jppr.2022.06.001.
20) Asogwa KK, Ibe AA. A Study of MHD Casson Fluid Flow over a Permeable Stretching Sheet with Heat and Mass Transfer. *Journal of Engineering Research and Reports*. 2020;16(2):10–25. Available from: https://doi.org/10.9734/JERR/2020/v16i217161.